SF2A 2019
P. Di Matteo, O. Creevey, A. Crida, G. Kordopatis, J. Malzac, J.-B. Marquette, M. N'Diaye, O. Venot (eds)

3D RECONSTRUCTION OF THE ENVIRONMENT OF THE RED SUPERGIANT μ CEP FROM NOEMA OBSERVATIONS OF THE CO V=0 J=2-1 LINE

M. Montargès[1], W. Homan[1], D. Keller[1], N. Clementel[1], S. Shetye[1,2], L. Decin[1], G. M. Harper[3], P. Royer[1], J. M. Winters[4], T. Le Bertre[5,6] and A. M. S. Richards[7]

Abstract. Red supergiant stars are surrounded by a circumstellar environment containing gas and dust. It is created as the star loses its mantle via an unknown mass-loss process. Refining our knowledge of the morphology and physics of such environments is critical to understanding the processes that drive this mass loss. This mass loss phenomenon is also a key element to determine the fate of the star, as it directly determines the mass of the supernova progenitor and hence of the remaining compact object. We present the result of our observations of the CO $v = 0$ $J = 2 - 1$ emission line of the RSG μ Cep with the NOEMA interferometer at the arcsec angular resolution scale (~ 500 au at the star distance). Using a combination of 3D deprojection and 3D radiative transfer modeling, we show that at least 25% of the mass loss is due to clumps, randomly arranged in space and emitted episodically by the star.

Keywords: circumstellar matter, stars: imaging, stars: individual: μ Cep, stars: mass-loss, supergiants, radio lines: stars

1 Introduction

Cool evolved stars are important contributors to the chemical enrichment of the interstellar medium thanks to their important mass loss (10^{-8} to $10^{-4}\,M_\odot$ yr^{-1}). The elements forged within their cores are transported to their surface via powerful convective motions. Within their stellar winds, these elements are cooling to form molecules and dust grains that will be pristine building blocks for future stellar system and life precursors. Massive stars ($M_{ini} > 8\,M_\odot$) evolve into red supergiants (RSG). The mass loss of these stars is not completely understood: the launching mechanism, the dust condensation processes and location, and the role of their chromosphere are still unknown.

2 Observations

We observed the RSG star μ Cep using NOEMA on 2015 December 2 and 2016 March 24 in the 7C (3.4h on source) and 7B (2.6h on source) configurations, respectively. The narrow band backend was used to provide line data in both polarizations with a 160 MHz bandwidth unit. For the CO $J = 2 - 1$ line at 230.538 GHz, this resulted in a spectral resolution of 0.81 km s^{-1} over a range of ± 90 km s^{-1}. To produce the continuum at 231.276 GHz, we used the Wideband Express (WideX) backend with a 4 GHz bandwidth to select line-free channels. The data were reduced and calibrated using the GILDAS package*. We then performed a self-calibration of the line data in the (u, v) plane using the continuum data. The noise level (σ) was 0.71 mJy beam^{-1} in the continuum map and $2.03 - 4.70$ mJy beam^{-1} in the line channel maps. Further details on the data acquisition, reduction and calibration can be found in Montargès et al. (2019, hereafter M19).

[1] Institute of Astronomy, KU Leuven, Celestijnenlaan 200D B2401, 3001 Leuven, Belgium
[2] Institute of Astronomy and Astrophysics, Université libre de Bruxelles, B-1050 Bruxelles, Belgium
[3] Center for Astrophysics and Space Astronomy, University of Colorado, Boulder, CO 80309, USA
[4] Institut de Radioastronomie Millimétrique, 300 rue de la Piscine, 38406, Saint Martin d'Hères, France
[5] LERMA, Observatoire de Paris, PSL Research University, CNRS, UMR 8112, 75014, Paris, France
[6] Sorbonne Universités, UPMC Univ. Paris 06, UMR 8112, LERMA, 75005, Paris, France
[7] Jodrell Bank Centre for Astrophysics, School of Physics and Astronomy, University of Manchester, Manchester M13 9PL, UK
*http://www.iram.fr/IRAMFR/GILDAS

3 Data analysis

3.1 Continuum

Figure 1 shows the self-calibrated continuum from the NOEMA data. Only the central source is detected above 3σ, it remains unresolved. Its point flux density is 39.67 ± 7.93 mJy. Using an updated model from Harper et al. (2001), M19 showed that most of the continuum emission comes from the compact free-free emission of the RSG chromosphere.

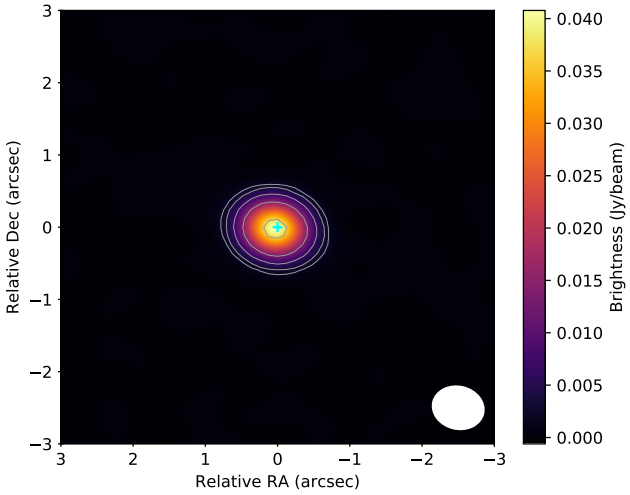

Fig. 1. Self-calibrated continuum map of μ Cep centred at 231.276 GHz. The synthesized beam is represented by the white ellipse at the bottom right corner of the image. The cyan cross marks the position of the star. The contour levels are 3, 5, 10, 20, and 50 times the noise rms (M19).

3.2 Line data

The self-calibrated, continuum subtracted channel maps of the CO v=0, J=2-1 line at 230.538 GHz are represented on Fig. 2. In each map, the gaseous circumstellar environment of the star appears very clumpy. The clumps are identified in detail in M19. In the Local Standard of Rest Kinematic (LSRK) frame the velocity of the star is $v_\star = 32.7 \pm 0.1$ km s^{-1}. For $v_{\rm LSRK} > 7.5$ km s^{-1}, the environment presents a "classical" shape surrounding the star with clumps belonging to a circumstellar envelope or detached from it. However, for $v_{\rm LSRK} < 7.5$ km s^{-1}, the environment is dominated by two bright clumps, C1 on the South-West at 1.80 arcsec from the star (1.15 kau at the distance of μ Cep determined to be 641 pc in M19) and C2 roughly centered at the star position.

3.3 3D deprojection and 3D radiative transfer modeling

In order to better understand the characteristics of the circumstellar environment of μ Cep, we used two complementary approaches. First, we deprojected the CO intensity map according to the method used by Guélin et al. (2018). This allows to have a real 3D representation of the material around the star, instead of channel maps. Therefore, it gives access to the full position (x, y, z) of the clumps relative to the star, and to their size. We assumed a constant radial outflow as our beam size of 0.92×0.72 arcsec (590×462 au at 641 pc) resolves only marginally the non-spherical accelerating region (Harper et al. 2001; Höfner et al. 2016). We chose a slow wind velocity of $v_\infty^{\rm slow} = 25.0$ km s^{-1} for the material in channel maps whose velocities are in the interval $v_\star \pm v_\infty^{\rm slow}$, and a faster wind velocity $v_\infty^{\rm fast} = 43.0$ km s^{-1} otherwise. These velocities are determined from the width of the red and blue line wings of the line respectively. The result of this deprojection is presented in a movie (Fig. 3)

The characteristics of the clumps derived from this deprojection are used as input for a 3D radiative transfer modeling using the code LIME (Brinch & Hogerheijde 2010). The model consists in the different clumps as well as a smooth continuous wind (for more details, see M19). The synthetic emission distribution of the clumps is

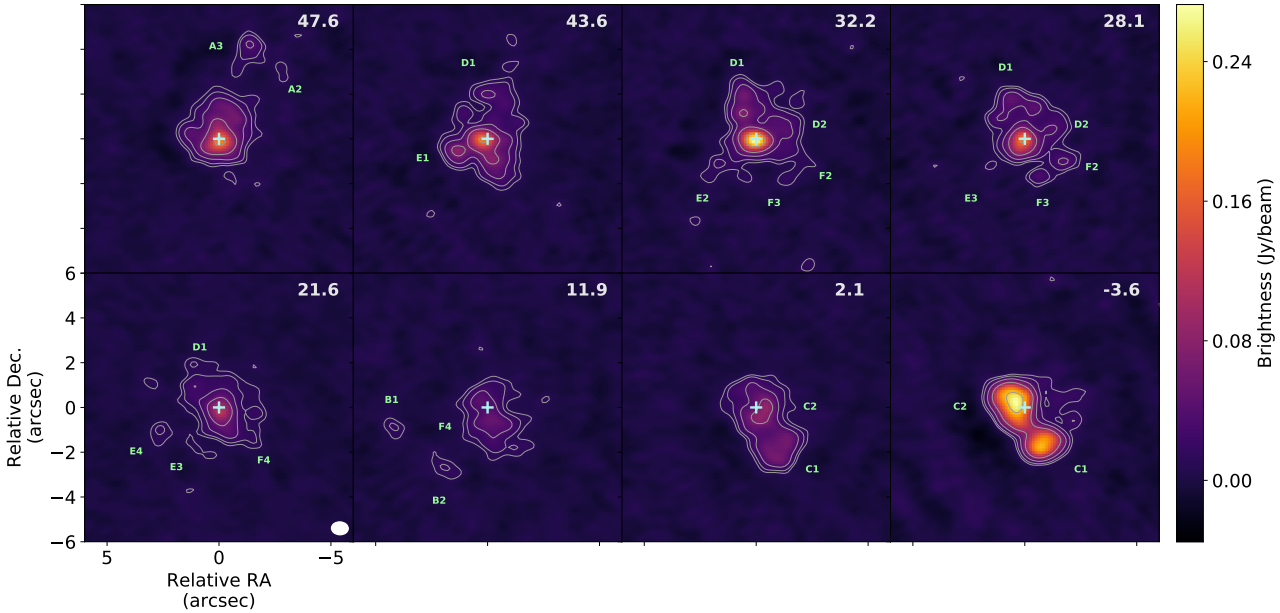

Fig. 2. Sample of the continuum subtracted channel maps of μ Cep obtained with NOEMA and centered at 230.538 GHz. The LSRK (LSR kinematic frame) radial velocity in km s^{-1} is expressed in the top right corner of each map. The LSRK velocity of the star is 32.7 ± 0.1 km s^{-1}. The synthesized beam is represented by the white ellipse at the bottom right corner of the first image of the last row. On each map, the pale blue cross marks the position of the star at the (0, 0) relative coordinates. The contour levels are 3, 5, 10, 20, and 50 times the noise rms of the respective channel. The clumps are identified by the pale green labels. (M19)

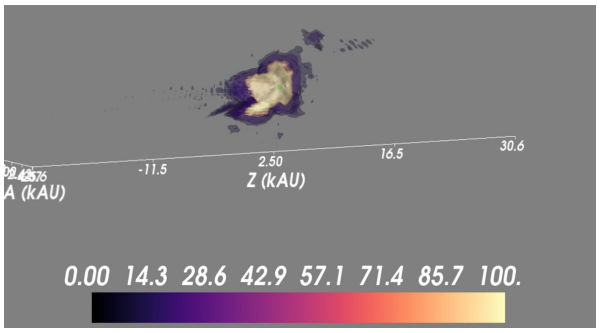

Fig. 3. Three-dimensional rendering of the deprojection of μ Cep's environment in the CO J=2-1 line. A movie is available online at: `https://frama.link/muCep3D`. (M19)

reproducing well the emission from the observed clumps. However, we had difficulties to reproduce the emission located in the central beam area where the smooth outflow component should be dominant, this is particularly the case in the blue wing. This could be due to the presence of unresolved inhomogeneities that cannot be approximated by a smooth outflow. All the clumps except for C1 appear to be optically thin.

The modeling gave us access to the mass of the individual clumps. By using their distance from the central star and the wind speed, we are able to deduce their contribution to the mass loss: $(4.9 \pm 1.0) \times 10^{-7}\,\mathrm{M}_\odot\ \mathrm{yr}^{-1}$. This value is strongly dependent on the fractional CO abundance we assumed. In particular, according to Huggins et al. (1994) the dominant atomic form of carbon in the circumstellar environment could lead to a CO abundance ten times lower. For the optically thin clumps, this translates in an increase by a factor ten of their mass. For the optically thick C1, if the same process drives the ejection of all the clumps, we can assume that the mass of C1 would also scale inversely to the CO/H_2 ratio. Therefore the mass loss due to the clump would be $(4.9 \pm 1.0) \times 10^{-6}\,\mathrm{M}_\odot\ \mathrm{yr}^{-1}$. This value is close to the total mass-loss rate determined by Shenoy et al. (2016), meaning that most of the mass loss would then occur through the clumps.

4 Conclusions

We obtained high angular resolution observations of the circumstellar environment of the RSG μ Cep in the CO $J = 2 - 1$ line. The material around the star is distributed in several clumps, two of them being particularly prominent in the blue channels. From a 3D deprojection to properly determine the position and size of the clumps, and a 3D radiative transfer modeling, we were able to determine their mass and therefore their contribution to the mass loss of the star. Depending on the CO fractional abundance, we estimate that at least 25% of the mass loss is contributed by the clumps, the rest being due to a smooth and continuous outflow. However, it is also possible that all the mass loss could be due to the clumps and the smooth spherical outflow non-existent. Mauron (1997) observed the environment of μ Cep from 5 to 60″ in the resonant KI lines at 770 nm. He finds evidence of clumps with typical sizes $\sim 2''$. These results agree with ours and suggest that the inhomogeneities that we discovered in the CO line may survive for 10^4 years. The random distribution of the clumps around the star as well as their different distances are arguments in favor of an episodic mechanism launching the mass loss from randomly distributed regions on the photosphere.

This work is based on observations carried out under project number W15BL with the IRAM NOEMA Interferometer. IRAM is supported by INSU/CNRS (France), MPG (Germany) and IGN (Spain). We are grateful to the IRAM/NOEMA staff at the Plateau de Bure observatory for the successful execution of the observations. This project has received funding from the European Union's Horizon 2020 research and innovation program under the Marie Skłodowska-Curie Grant agreement No. 665501 with the research Foundation Flanders (FWO) ([PEGASUS]^2 Marie Curie fellowship 12U2717N awarded to M.M.). LD, WH, DK, and NC acknowledge support from the ERC consolidator grant 646758 AEROSOL. We used the SIMBAD and VIZIER databases at the CDS, Strasbourg (France)[†], and NASA's Astrophysics Data System Bibliographic Services. This research made use of Matplotlib (Hunter 2007), Astropy[‡], a community-developed core Python package for Astronomy (Astropy Collaboration et al. 2013), and Uncertainties[§]: a Python package for calculations with uncertainties.

References

Astropy Collaboration, Robitaille, T. P., Tollerud, E. J., et al. 2013, A&A, 558, A33

Brinch, C. & Hogerheijde, M. R. 2010, A&A, 523, A25

Guélin, M., Patel, N. A., Bremer, M., et al. 2018, A&A, 610, A4

Harper, G. M., Brown, A., & Lim, J. 2001, ApJ, 551, 1073

Höfner, S., Bladh, S., Aringer, B., & Ahuja, R. 2016, A&A, 594, A108

Huggins, P. J., Bachiller, R., Cox, P., & Forveille, T. 1994, ApJ, 424, L127

Hunter, J. D. 2007, Computing In Science & Engineering, 9, 90

Mauron, N. 1997, A&A, 326, 300

Montargès, M., Homan, W., Keller, D., et al. 2019, MNRAS, 485, 2417

Shenoy, D., Humphreys, R. M., Jones, T. J., et al. 2016, AJ, 151, 51

[†]Available at `http://cdsweb.u-strasbg.fr/`

[‡]Available at `http://www.astropy.org/`

[§]Available at `http://pythonhosted.org/uncertainties/`